Zagazig University Medical Journal
www.zumj.journals.ekb.eg
https://doi.org/10.21608/zumj.2024.321384.3582 Volume 30, Issue 9, December. 2024
Manuscript id: ZUMJ-2409-3582
Doi:10.21608/ZUMJ.2024.321384.3582
ORIGINAL ARTICLE

Exploring the Cytoprotective Role of Liraglutide in Non-Alcoholic Fatty Liver Disease Experimentally Induced in the Rat Model (Histological and Biochemical Study)

Sahar F Shaban[1], Dalia A Mohamed[1], Aya Ismael Elsayed Mahmoud[2]*, Heba Mohamed Abdel-aziz[1]
[1] Histology and Cell Biology Department, Faculty of Medicine, Zagazig University
[2] Histology and Cell Biology Department, Faculty of Medicine, Suez University

***Corresponding author:**
Aya Ismael Elsayed Mahmoud

Email :
aya.i021@medicine.zu.edu.eg

Submit Date 18-09-2024
Revise Date 02-10-2024
Accept Date 08-10-2024

ABSTRACT

Background: Nonalcoholic fatty liver disease (NAFLD) is a widespread health issue and regarded as the most prevalent condition affecting the liver worldwide. Liraglutide, a glucagon-like peptide-1 receptor agonist, is a promising and innovative drug. Our study aimed to investigate the protective role of liraglutide in experimentally induced NAFLD in the rat model.

Methods: Forty healthy adult male albino rats were used, they were assigned to 3 main groups: Group I (Control group) which was subdivided into two equal subgroups, Group II (High-fat diet group) which rats were given a fatty diet for 12 weeks and Group III (High-fat diet +liraglutide group) in which rats were fed with high fatty diet in the same way as group II in concomitant with liraglutide that was injected subcutaneously daily (0.2 mg/kg) for 12 weeks. Blood samples and liver tissues were collected and assayed for biochemical, histological, and immunohistochemical studies.

Results: The high-fat diet group exhibited a significant increase in body mass index, abdominal circumference, serum ALT, AST, and serum lipid profile levels. Additionally, hepatic destructive changes were observed such as hepatocellular vacuolation, apoptosis, and congested blood vessels, along with a significant increase in the area percentage of collagen fibers, caspase 3 immunoreactions, and the number of GFAP immunoreactivity of hepatic stellate cells. These distortions were confirmed by ultrastructural assessment. In contrast, the high-fat diet +liraglutide group exhibited normal BMI, AC, ALT, AST, and lipid profiles with preservation of the liver histoarchitecture.

Conclusion: NAFLD significantly affects hepatic cytoarchitecture and biochemical parameters, leading to apoptosis and fibrosis. Liraglutide administration with a high-fat diet can protect the liver from these changes.

Keywords: NAFLD; Liraglutide; Caspase 3; GFAP

INTRODUCTION

The modern rushing life has induced a type of unhealthy lifestyle that depends mainly on junk food and high-fat diets (HFD). HFD induces a wide spectrum of metabolic alterations in the human body. These changes often include increasing adiposity, particularly visceral fat deposition **[1]**. Moreover, HFD consumption has been linked with impaired glucose homeostasis, manifested by insulin resistance and glucose intolerance. Thus those individuals predispose to the development of type 2 diabetes and several health problems. These complications can contribute to cardiovascular diseases, obesity and nonalcoholic fatty liver disease **[2].**

The term nonalcoholic fatty liver disease (NAFLD) refers to buildup of fats in the liver that is not brought on by excessive alcohol consumption. It can advance from simple steatosis to cirrhosis and hepatocellular

cancer, as well as from steatohepatitis (NASH) to progressive fibrosis **[3].**

Huang et al. [4] mentioned that effective treatment options for NAFLD remain limited despite its growing global prevalence and clinical significance. This increases the need for novel therapeutic approaches. **Jeeyavudeen et al. [5]** suggested a promising direction of pharmacological agents aiming to control metabolic irregularities and liver conditions linked to NAFLD. Moreover, interventions such as dietary modifications, exercise regimens, and gene therapy can be tested to assess their efficacy in preventing or reversing NAFLD-related liver damage**.**

Liraglutide functions similarly to glucagon-like peptide-1 (GLP-1), an incretin hormone released by L cells in the ileum after ingesting carbs and lipids. The body reacts to the medicine in different ways. It reduces blood sugar levels by promoting the release of insulin and suppressing the secretion of glucagon in reaction to glucose and enhancing glucose balance. Furthermore, its ability to slow down digestion leads to reduced food intake **[6].**

Liraglutide is recognized as a therapeutic agent for the management of type 2 diabetes mellitus (T2DM) patients. It has beneficial impacts on various organs, including the pancreas, heart and kidneys. The underlying mechanisms potentially reduce body weight and decrease lipid synthesis. It also induces autophagy, and free fatty acid β-oxidation **[7].** Building upon preclinical and clinical evidence supporting the efficacy of liraglutide in improving liver pathologies, this study used biochemical, histological, and immunohistochemical studies to investigate how liraglutide protects against experimentally generated NAFLD in adult male albino rats.

METHODS

Diets:

- Balanced diet: Normal chow diets (obtained from Al Wady Company, Cairo, Egypt) were in the form of pellets with the following constituents: 17% protein, 4.9% fat, 68.16% carbohydrates, 2% choline chloride, 1% vitamin mixture, 3.5% salt mixture, and 3.44% fiber **[8].**

-High-fat Diet (HFD): Consists of 20% carbs, 20% protein, and 60% fat. Based on the total caloric content of 5243 kcal/kg, each gram of the ingredients contained 5.24 kcal and 232 mg of cholesterol. Pellets from Research Diets, Inc. (D12492 diet), New Brunswick, NJ, 08901 USA, were used **[9, 10].**

Chemicals:

-Liraglutide: obtained as injectable pens 3ml (6mg/ml) (Novo Nordisk company, Denmark). For 12 weeks, a daily subcutaneous injection at a dose of 0.2 mg/kg was administered **[11].**

Anti-Caspase 3 monoclonal antibody: A rabbit monoclonal antibody of (anti-caspase 3) class IgG. Universal kits for caspase 3 were obtained from Lab Vision Laboratories (CAT.#14751).

-Anti-glial fibrillary acidic protein (GFAP) monoclonal antibody: A rabbit monoclonal antibody of anti-glial fibrillary acidic protein (anti-GFAP) class IgG. universal kits for GFAP manufactured by Biogen Inc. (Cambridge, Massachusetts, USA) were obtained from Dako company (Egypt) (CAT. #FNab03426)

Animals:

In this study, forty adult healthy male albino rats weighing 180–200 grams and 10–12 weeks of age were utilized. The animals were sourced from the breeding facility at the Faculty of Medicine, Zagazig University. All experimental methods were carried out following the institutional animal care guidelines and ethical committee of the Faculty of Medicine, Zagazig University (IACUC approval: ZU-IACUC/3/F/114/2023).

Experimental design:

Animals were classified into 3 main groups:

Group I (Control group): comprised twenty adult male albino rats that were divided into two equal subgroups of ten rats each**:**

Subgroup Ia: Rats received a balanced diet till the end of the experiment.

Subgroup Ib: Rats were injected with liraglutide subcutaneously for 12 weeks at a dose of 0.2 mg/kg/day **[11].**

Group II (HFD group): Included ten rats that were fed HFD ad libitum for 12 weeks **[9, 10].**

Group III (HFD + Liraglutide group): Included ten rats that received the same HFD as group II along with injected with liraglutide subcutaneously for 12 weeks at a dose of 0.2 mg/kg/day **[11].**

Methods

General observation: The animals underwent weighing, and their nose-to-anus lengths were recorded to determine the body mass index (BMI) utilizing the equation [body weight (g) / length² (cm²)] **[12].** This process involved calculating the initial BMI at the beginning of the experiment and the final BMI at its end. The data for both initial and final BMI were then analyzed statistically.

The abdominal circumference (AC) was assessed in the most prominent area of the rat's abdomen **[13].**

Measurements of initial AC were collected from the animals at the beginning of the experiment, while final AC measurements were taken at the end of the experiment. Both initial and final AC data underwent statistical analysis.

Biochemical study: Using capillary tubes, Blood samples were collected from the orbital veins at the end of the experiment to evaluate liver functions (serum ALT and AST) and lipid profiles (TC, TG, HDL, LDL). Alanine transaminase (ALT) and Aspartate transaminase (AST) were assessed using the Rat Aspartate aminotransferase ELISA Kit, (MyBiosource, UK), CAT no MBS2. Total cholesterol, HDL, and LDL were determined using the Quantitative Colorimetric Determination method (CELL BIOLABS, INC., USA) CAT no STA-391. Triglycerides (TGs) were determined using the colorimetric assay of serum triglycerides, (CELL BIOLABS, INC., USA) CAT no STA-396. The rats were fasted for up to 12 hours for accurate lipid profile examination **[14]**. Every sample was measured at the Biochemistry Department, Faculty of Medicine, Zagazig University.

Histological study: The animals from all groups were anesthetized using ether inhalation. Their thoracic cages were then opened, and they were perfused intracardially with 2.5% glutaraldehyde in cacodylate buffer. After that, the livers were removed and the left lobes were obtained. The liver specimens were carefully dissected for light and electron microscopic study.

a- Light microscopic study:

Liver specimens($1cm^3$) were promptly preserved in formalin 10% buffer, dried, embedded in paraffin, and sectioned into 5 µm paraffin sections. They were then subjected to staining with hematoxylin & eosin (H&E) to reveal the general histological structures and were also treated with Sirius red stain to determine the distributions of collagen fibers **[15].**

b- Transmission electron microscope (TEM) study [16]: Liver specimens ($1mm^3$) were fixed in 2.5% glutaraldehyde. They were then washed in 0.1 M phosphate buffer and post-fixed in 1% osmium tetroxide. The specimens were implanted in epoxy resin after being dehydrated. Semithin sections (1µm) were stained with toluidine blue and examined with a light microscope. Ultrathin sections (50 nm) were cut, stained, examined, and photographed by TEM (1200 EXII) Electron Microscope Unit, Faculty of Agriculture, Mansoura University.

Immunohistochemical Study [15]: 5 µm paraffin sections underwent deparaffinization, rehydration, and treatment with 3% hydrogen peroxide to inhibit endogenous peroxidase activity. For 30 minutes, Antigen retrieval was performed at a temperature of 95°C using a citrate buffer with a concentration of 0.01 M and a pH of 6.0. The sections were treated with rabbit monoclonal antibodies diluted 1:400 for anti-Caspase-3 and 1:500 for anti-GFAP for a whole night at 4°C. Then the sections were treated with an avidin-biotin-peroxidase complex and biotinylated horse anti-mouse IgG. The reaction was observed using diaminobenzidine tetrahydrochloride (DAB) solution and Mayer's hematoxylin counterstaining. Phosphate-buffered saline was used in place of the primary monoclonal antibody to create the negative control sections.

Morphometrical study: Sections stained with Sirius red and immune-stained sections from all studied groups were analyzed. Using Leica DM500 image analyzer computer system (Switzerland) at Human Anatomy and Embryology Department Analysis Unit, Faculty of Medicine, Zagazig University. The area percentage of the collagen distribution stained by Sirius red, as well as the area percentage of caspase 3 immunoexpressions and cell count of GFAP immunoreactive positive cells, were examined at magnification power x400. For each parameter, 10 non-overlapping fields were selected.

Statistical analysis:

The data collected for BMI, AC, biochemical study and morphometrical results underwent statistical analysis. The Statistical Package for the Social Sciences (SPSS) version 20.0 software was used. To compare the means of different groups, the data were presented as mean ± standard deviation (SD) and analyzed using one-way analysis of variance (ANOVA).

RESULTS

General Observations:

-During the experimental period, 2 deaths in rats of the HFD group were documented.

-Quantities of food consumed by rats in the HFD group were more when compared to the remaining groups.

-Data obtained from all control subgroups revealed similar results and they showed no statistically significant results. Thus, subgroup Ia was chosen as representative for the control group.

The initial BMI of the experimental groups did not show any statistically significant differences ($p>0.05$). On the other hand, the final BMI of the HFD group, showed a highly significant increase when compared to control and HFD + liraglutide groups ($p\leq0.001$) **(Table 1, Figure A1).**

The initial AC of the experimental groups did not show any statistically significant differences ($p>0.05$). Whereas the final AC of the HFD group, showed a highly significant increase when compared to the control and HFD + liraglutide groups ($p\leq0.001$) **(Table 1, Figure A2).**

Biochemical results:

-A statistical evaluation of ALT and AST showed a highly significant increase in the HFD group compared to control and HFD+ liraglutide groups ($p\leq0.001$). Furthermore, no significant difference was detected between the HFD + liraglutide group and the control group($p>0.05$) (**Table 1, Figure A3).**

-When comparing the HFD group to the control and HFD + liraglutide groups, statistical analysis of TC, TG, and LDL showed a highly significant increase in these parameters ($p\leq0.001$). Furthermore, no significant difference was observed between the HFD + liraglutide group and the control group ($p>0.05$). In contrast, there was a highly significant decrease in HDL in the HFD group when compared to the control and HFD + liraglutide groups ($p\leq0.001$). Furthermore, no significant difference was observed between the HFD + liraglutide group and the control group ($p>0.05$) (**Table 1, Figure A4).**

Histological results:

Hematoxylin and eosin (H&E) (Figure 1):

The control group showed liver tissues had normal architecture of classic hepatic lobules. From the central veins tightly packed hepatocyte cords radiated with portal regions identified at their corners **(Figure. 1a)**. The hepatocytes had polyhedral appearances with rounded vesicular nuclei and acidophilic cytoplasm. Blood sinusoids with endothelium lining them in between the hepatocytes and binucleated hepatocytes were also seen **(Figure 1b)**. The portal areas contained branches of portal veins, bile ducts, and hepatic arteries embedded in loose connective tissues **(Figure 1c)**. While, in the HFD group, many hepatocytes had multiple vacuoles in their cytoplasm and some of them had darkly stained nuclei and deeply acidophilic cytoplasm. The blood sinusoids in between hepatocytes appeared dilated. Moreover, dilated congested branches of portal veins and proliferated several bile ducts were observed in the portal areas **(Figures 1d &1e).** In the HFD+ liraglutide group, the hepatocytes appeared polyhedral shapes with vesicular nuclei and acidophilic cytoplasm. Some hepatocytes had dark nuclei and others were binucleated. There were also observations of slightly dilated blood sinusoids and portal regions, accompanied by mildly congested branches of the portal vein and bile ducts **(Figures 1f &1g).**

Sirius red stains (Figure 2):

The control group displayed sections showing few collagen fibers encircling the central veins, hepatic sinusoids, and portal regions **(Figures 2a& 2b).** In the HFD group, abundant collagen fibers were observed around the same structures **(Figures 2c &2d).** Moderate collagen fibers were seen around central veins, hepatic sinusoids, and portal regions in the HFD+ liraglutide group **(Figures 2e&2f).**

Immunohistochemical results (Figure 3):

Immunohistochemical stained sections showed mild reactions for caspase 3 in the cytoplasm of a few hepatocytes (**Figure 3a)** and mild reactions of GFAP in a few hepatic stellate cells (HSCs) (**Figure 3d).** In the HFD group, immunostained sections of caspase 3 showed intense reactions in the cytoplasm of most hepatocytes (**Figure 3b)** and also intense reactions for GFAP in numerous (HSCs) (**Figure 3e**). In the HFD+ liraglutide group, caspase 3 showed moderate reactions in some hepatocytes' cytoplasm (**Figure 3c)** and also moderate reactions of GFAP in some (HSCs) (**Figure 3f).**

Toluidine blue stained semithin sections (Figure 4):

Polyhedral hepatocytes with vesicular nuclei and visible nucleoli were observed in the control group. Their cytoplasm included a large number of basophilic granules. Blood sinusoids with their endothelial lining and Von Kupffer cells were also observed **(Figure 4a).** In the HFD group, the hepatocytes appeared with apparently small nuclei and few basophilic cytoplasmic granules. Multiple cytoplasmic vacuoles of variable sizes and dilated blood sinusoids were also observed **(Figure 4b).** HFD +liraglutide group revealed hepatocytes with vesicular nuclei, visible nucleoli, and basophilic cytoplasmic granules. Dilated blood sinusoids and Von Kupffer cells were also seen (**Figure 4c).**

***Electron microscopic examinations*:**

The control group's ultrathin sections revealed hepatocytes with euchromatic nuclei and noticeable nucleoli. The cytoplasm was rich in mitochondria as well as cisternae of both rough and smooth endoplasmic reticulum along with glycogen granules. Additionally, bile canaliculi were observed between the hepatocytes. Within the Disse spaces, located between hepatocytes and blood sinusoids, the hepatocytes exhibited numerous microvilli and sinusoids had red blood cells (**Figures 5a&5b&5c)**.

In the HFD group, hepatocytes appeared with heterochromatic nuclei and some hepatocytes had shrunken apoptotic nuclei. The cytoplasm showed lipid droplets, swollen mitochondria with disrupted cristae,

and areas of rarefaction. In Disse spaces, many collagen fibers were detected as well as hepatic stellate cells with lipid droplets in their cytoplasm and also hepatocytes exhibited few and disrupted microvilli (**Figures 6a&6b&6c&6d).**

The HFD+ liraglutide group showed hepatocytes with euchromatic nuclei and prominent nucleoli. There were mitochondria, dilated smooth endoplasmic reticulum, and a few areas of rarefication in their cytoplasm. In Disse spaces, hepatocytes exhibited numerous microvilli and some lipid droplets, and also hepatic stellate cells showed multiple lipid droplets in their cytoplasm. Bile canaliculi were also observed (**Figures 7a&7b&7c).**

Morphometrical results: (Table)

Statistical analysis of morphometrical results revealed a highly significant increase in the HFD group when compared to control and HFD+ liraglutide groups ($p \leq 0.001$) in the area percent of collagen fibers of Sirius red-stained sections **(figure B1),** and cell counts of HSCs of GFAP immune reactions **(figure B2)** and area percent of caspase 3 immune reactions **(figure B3).** However, when comparing the HFD group with the control and HFD + liraglutide group in the same parameters, there was no statistical difference ($p > 0.05$).

Table 1: Comparison between different studied groups using ANOVA test

Studied group / Items	control Mean ± SD	HFD Mean ± SD	HFD +liraglutide Mean ± SD	F Value	P value
Initial BMI(kg/m^2)	0.43±0.08	0.39±0.07	0.42±0.06	0.486	0.69*
Final BMI (kg/m^2)	0.53 ± 0.07	0.79 ± 0.06	0.55 ± 0.06	22.8	P١=0.001** P٢=0.5* P٣=0.002**
Initial abdominal circumference (cm)	15.93±0.38	15.97±0.38	16.15±0.29	0.639	*0.59
Final abdominal circumference (cm)	20.96 ± 0.3	24.6 ± 0.36	21.2 ± 0.2	207.4	P١=0.001** P٢=0.05* P٣=0.001**
ALT (U/L)	38.8 ± 0.77	161.7±4.1	44.19±9.6	5.1	P١=0.001** P٢=0.09* P٣=0.001**
AST (U/L)	145.8±5.58	173.4±42.9	154.2±35.1	3.4	P١=0.008** P٢=0.46* P٣=0.001**
TC (mmol/l)	75.89±1.31	164.0±3.3	80.8±9.6	533.475	P١=0.001** P٢=0.13* P٣=0.001**
TG (mmol/l)	48.49±1.12	111.5±6.6	52.1±6.14	3840.647	P١=0.001** P٢=0.08* P٣=0.001**
HDL(mmol/l)	42.49±0.79	25.44±0.6	41.9±1.1	511.834	P١=0.001** P٢=0.19* P٣=0.001**
LDL(mmol/l)	23.63±1.73	104.3±30.3	26.3±4.1	58.421	P١=0.001** P٢=0.07* P٣=0.001**
Area% Sirius red	1.98±0.2	12.67±2.0	2.82±0.41	244.932	P١=0.001** P٢=0.083* P٣=0.001**

Studied group / Items	control Mean ± SD	HFD Mean ± SD	HFD +liraglutide Mean ± SD	F Value	P value
Area% of caspase 3 immunoreactions	0.35±0.23	15.67±2.48	0.45±0.14	835.1	P١=0.001** P٢=0.877* P٣=0.001**
GFAP (cell count)	48.1±4.0	101.3±7.1	56.6±6.4	57.8	P١=0.001** P٢=0.05* P٣=0.001**

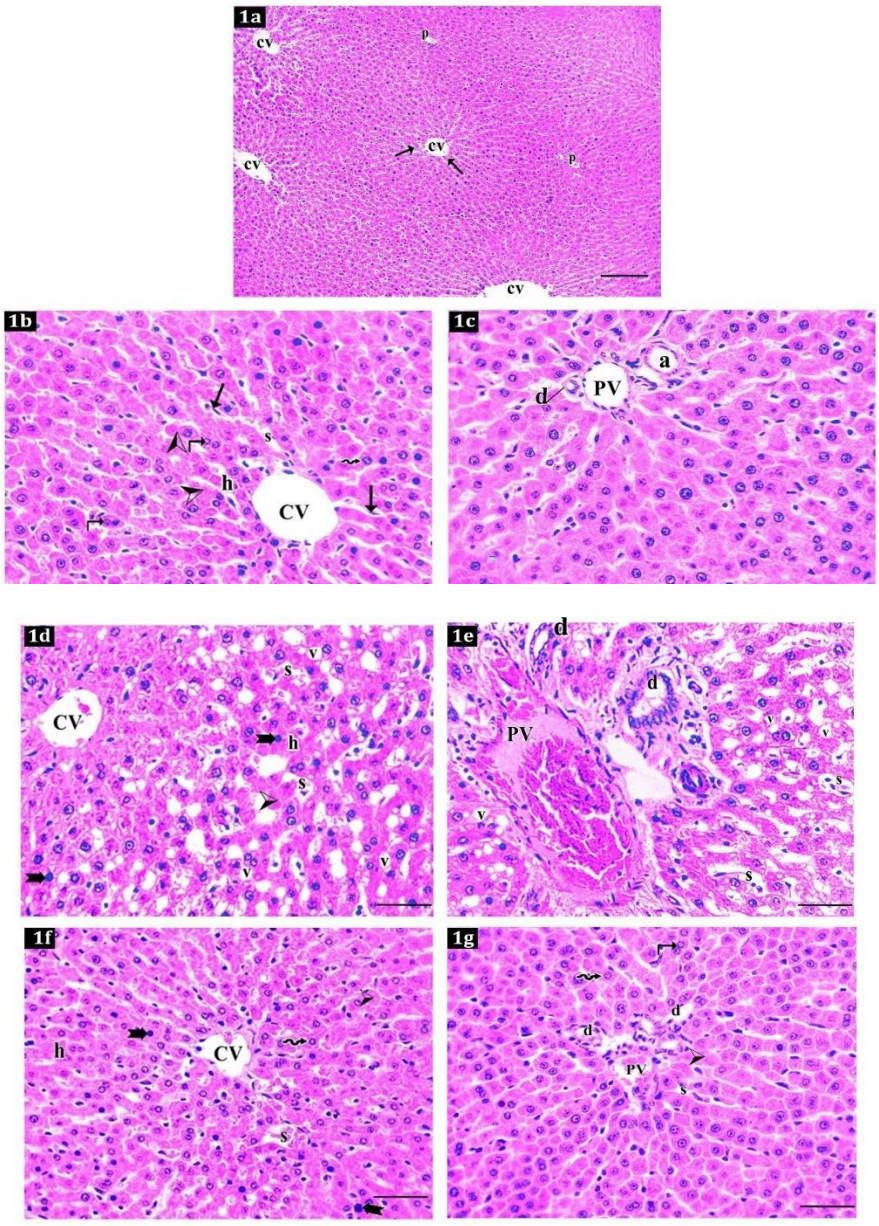

Figure (1): Photomicrographs of **H&E** stained sections in the left lobe of liver tissue of adult male albino rats:
1a: The control group showing classic hepatic lobules formed of tightly packed cords of hepatocytes **(arrows)** radiating from the central vein **(CV).** Portal areas **(P)** are observed at their corner. **(H&E, x100 - Scale bar 20 µm)**

1b: The control group shows hepatocytes **(h)** radiating from the central vein **(CV).** The hepatocytes appear polyhedral in shape with rounded vesicular nuclei **(zigzag arrow)** and acidophilic cytoplasm **(arrowheads)**. Blood sinusoids **(S)** with their endothelial lining **(arrows)** are detected. Binucleated hepatocytes are also seen **(curved arrows)**. **(H&E, x400 - Scale bar 30 µm)**
1c: The control group showing the portal area contains a branch of the portal vein **(PV)**, bile duct **(d),** and hepatic artery **(a)**. Cords of hepatocytes are also seen. **(H&E, x400 - Scale bar 30 µm)**
1d: The high-fat diet (HFD) group showing hepatocytes **(h)** have vacuolated cytoplasm **(V).** Other cells have darkly stained nuclei **(biffed arrows)** and deeply acidophilic cytoplasm **(arrowhead).** Dilated blood sinusoids **(S)** are also noticed. **(H&E, x400 - Scale bar 30 µm)**
1e: The high-fat diet group (HFD) showing portal area contains a dilated congested branch of the portal vein **(PV)** and several bile ducts **(d)**. Hepatocytes have vacuolated cytoplasm **(V)** with dilated blood sinusoids **(S)** in-betweens. **(H&E, x400 - Scale bar 30 µm)**
1f: The high-fat diet + liraglutide group shows polyhedral hepatocytes **(h)** radiating from the central vein **(CV)** and slightly dilated blood sinusoids **(S)**. Most hepatocytes have acidophilic cytoplasm **(arrowhead)** and rounded vesicular nuclei **(zigzag arrow).** Some hepatocytes appear with dark stained nuclei **(biffed arrow)**. **(H&E, x400- Scale bar 30 µm)**
1g: the high-fat diet + liraglutide group showing mild portal vein branch congestion **(PV)** and bile ducts **(d)** are noticed. slightly dilated blood sinusoids **(S).** Hepatocytes with vesicular nuclei **(zigzag arrow)** and acidophilic cytoplasm **(arrowhead)** and other hepatocytes are binucleated **(curved arrow). (H&E, x400- Scale bar 30 µm)**

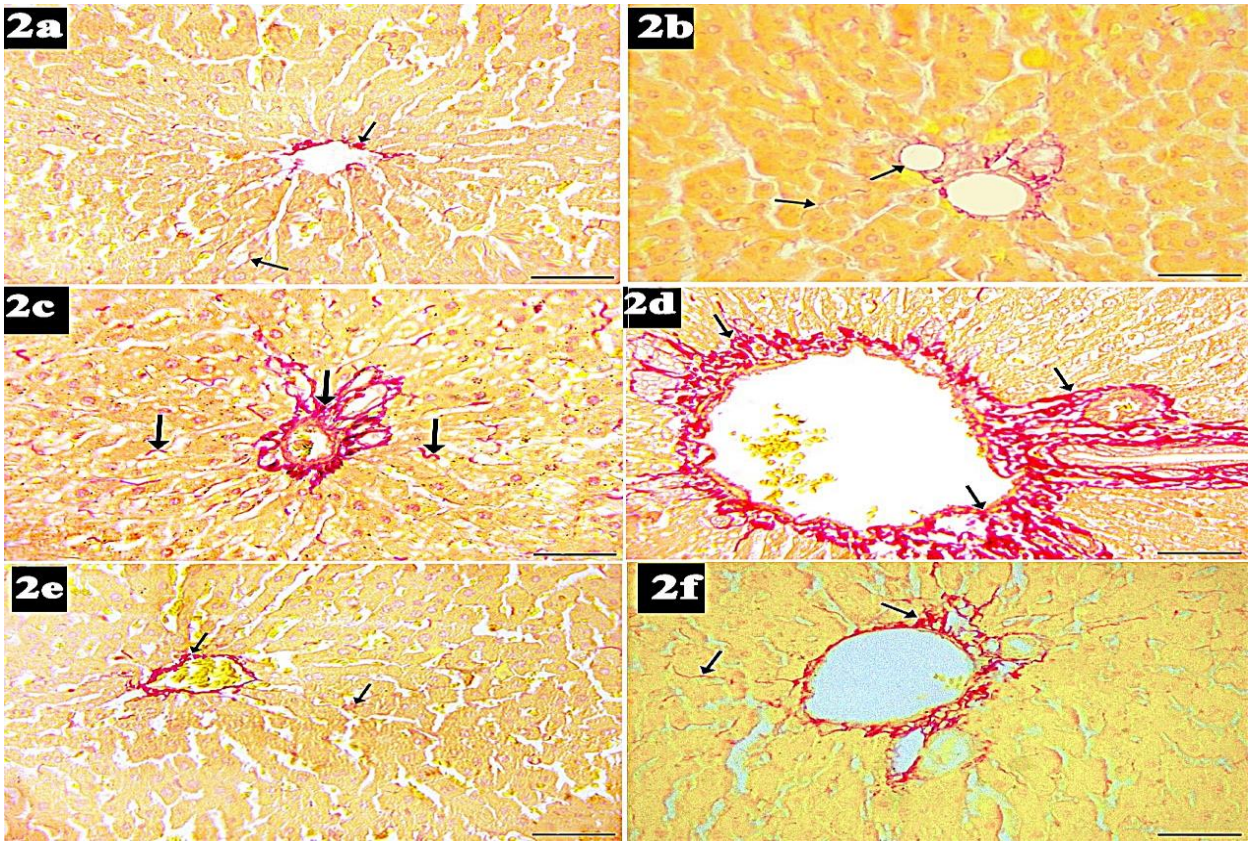

Figure 2: Photomicrographs of **Sirius red-stained** sections in the left lobe of liver tissue of adult male albino rats:
2a: The control group shows few collagen fibers **(arrows)** around the central vein and hepatic sinusoids. **(Sirius red Stain X 400 -Scale bar 30 µm)**
2b: The control group shows few collagen fibers **(arrows)** in the portal area and around hepatic sinusoids. **(Sirius red Stain X 400 -Scale bar 30 µm)**

2c: The high-fat group shows abundant collagen fibers **(arrows)** around the central vein and hepatic sinusoids. **(Sirius red x 400-Scale bar 30 µm)**
2d: The high-fat group shows abundant collagen fibers **(arrows)** around the portal area.
(Sirius red x 400-Scale bar 30 µm)
2e: The high-fat diet + liraglutide group exhibits moderate collagen fibers **(arrows)** around the central vein and hepatic sinusoids **(Sirius red Stain X 400-Scale bar 30 µm)**
2f: The high-fat diet + liraglutide group shows moderate collagen fibers **(arrows)** in the portal area and around hepatic sinusoids. **(Sirius red Stain X 400-Scale bar 30 µm)**

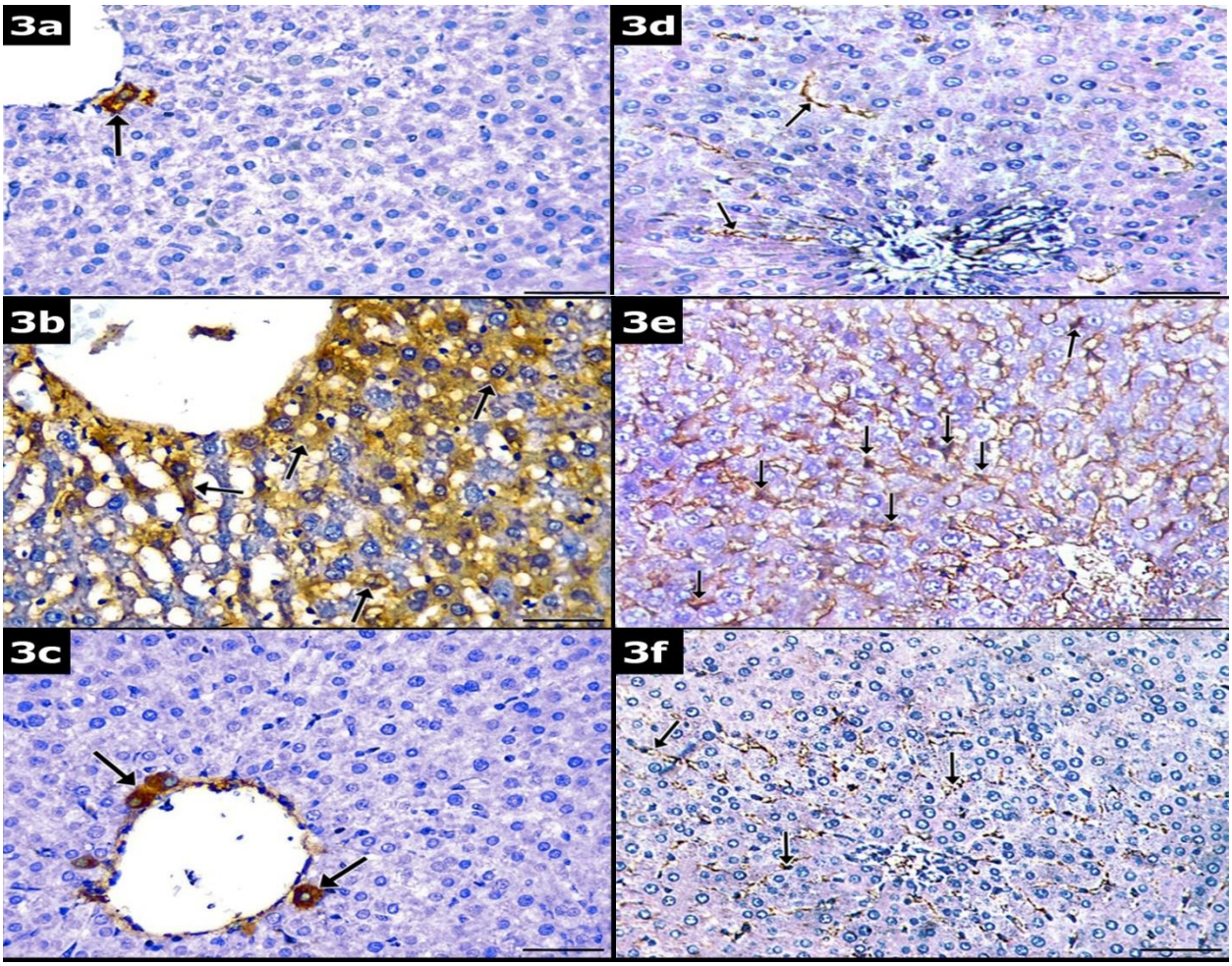

Figure (3) Photomicrographs of **immunohistochemically** stained sections in the left lobe of liver tissue of adult male albino rats
3a: The control group shows mild immunoreactions **(arrows)** for caspase 3 in the cytoplasm of a few hepatocytes. **(Immuno- peroxidase technique for caspase 3 ×400-Scale bar 30 µm)**
3b: The high-fat diet group exhibits intense immune- reactions **(arrows)** for caspase 3 in the cytoplasm of most of the hepatocytes. **(Immuno- peroxidase technique caspase 3 ×400 -Scale bar 30 µm)**
3c: The high-fat diet + liraglutide group showing moderate immunoreactions **(arrows)** for caspase 3 in the cytoplasm of a few hepatocytes. **(Immuno- peroxidase technique for caspase 3 ×400 -Scale bar 30 µm)**
3d: The control group shows mild immunoreactions **(arrows)** for glial fibrillary acidic protein in the cytoplasm of a few hepatic stellate cells (HSCs). **(Immuno- peroxidase technique for GFAP ×400 -Scale bar 30 µm)**
3e: The high-fat diet group showing intense immune- reactions **(arrows)** for glial fibrillary acidic protein in the cytoplasm of numerous hepatic stellate cells (HSCs) **(Immuno- peroxidase technique for GFAP ×400 -Scale bar 30 µm)**

3f: The high-fat diet + liraglutide group showing moderate immune reactions **(arrows)** in the cytoplasm of some hepatic stellate cells (HSCs) **(Immuno- peroxidase technique for GFAP ×400 -Scale bar 30 µm)**

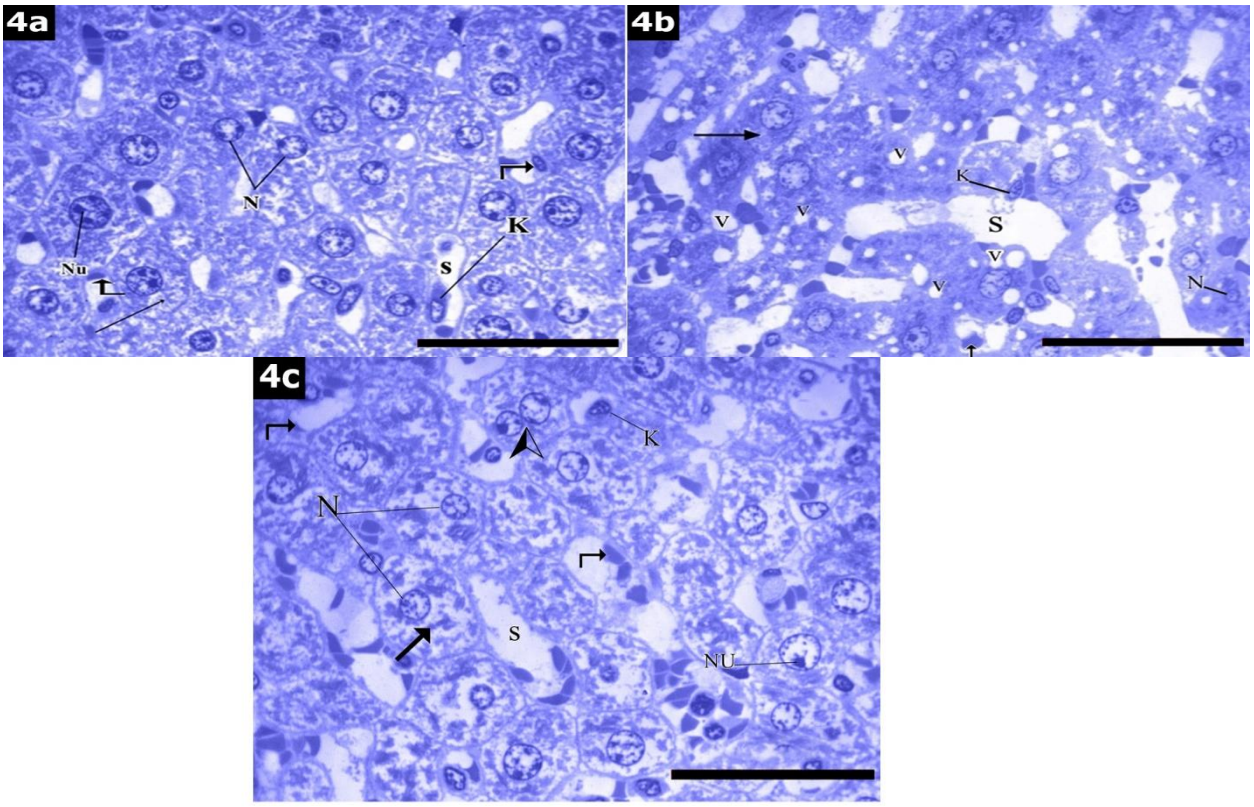

Figure (4): Photomicrographs of **Toluidine blue** stained semithin sections in the left lobe of liver tissue of adult male albino rats:
4a: The control group showing polyhedral hepatocytes with vesicular nuclei **(N)** and prominent nucleolus **(Nn)** and basophilic cytoplasmic granules **(arrow)** are detected. Blood sinusoids **(S)** with their endothelial lining **(curved arrow)** and Von Kupffer cells **(K)** are also observed. **(Toluidine blue x 1000 Scale bar 30 µm)**
4b: The high-fat group showing hepatocytes with apparently small nuclei **(N)** and few basophilic cytoplasmic granules **(arrow)** are recognized. Multiple cytoplasmic vacuoles of variable sizes **(V),** dilated blood sinusoids **(S),** and von Kupffer cells **(K)** are also observed. **(Toluidine blue x 1000 Scale bar 30 µm)**
4c: The high-fat diet+ liraglutide group shows hepatocytes with vesicular nuclei **(N)** and prominent nucleolus **(Nu)** and some of them are binucleated **(arrowhead).** Basophilic cytoplasmic granules **(arrow)** are recognized. Dilated blood sinusoids **(S)** with their endothelial lining **(curved arrow)** and Von Kupffer cells **(K)** are also observed. **(Toluidine blue x 1000 Scale bar 30 µm)**

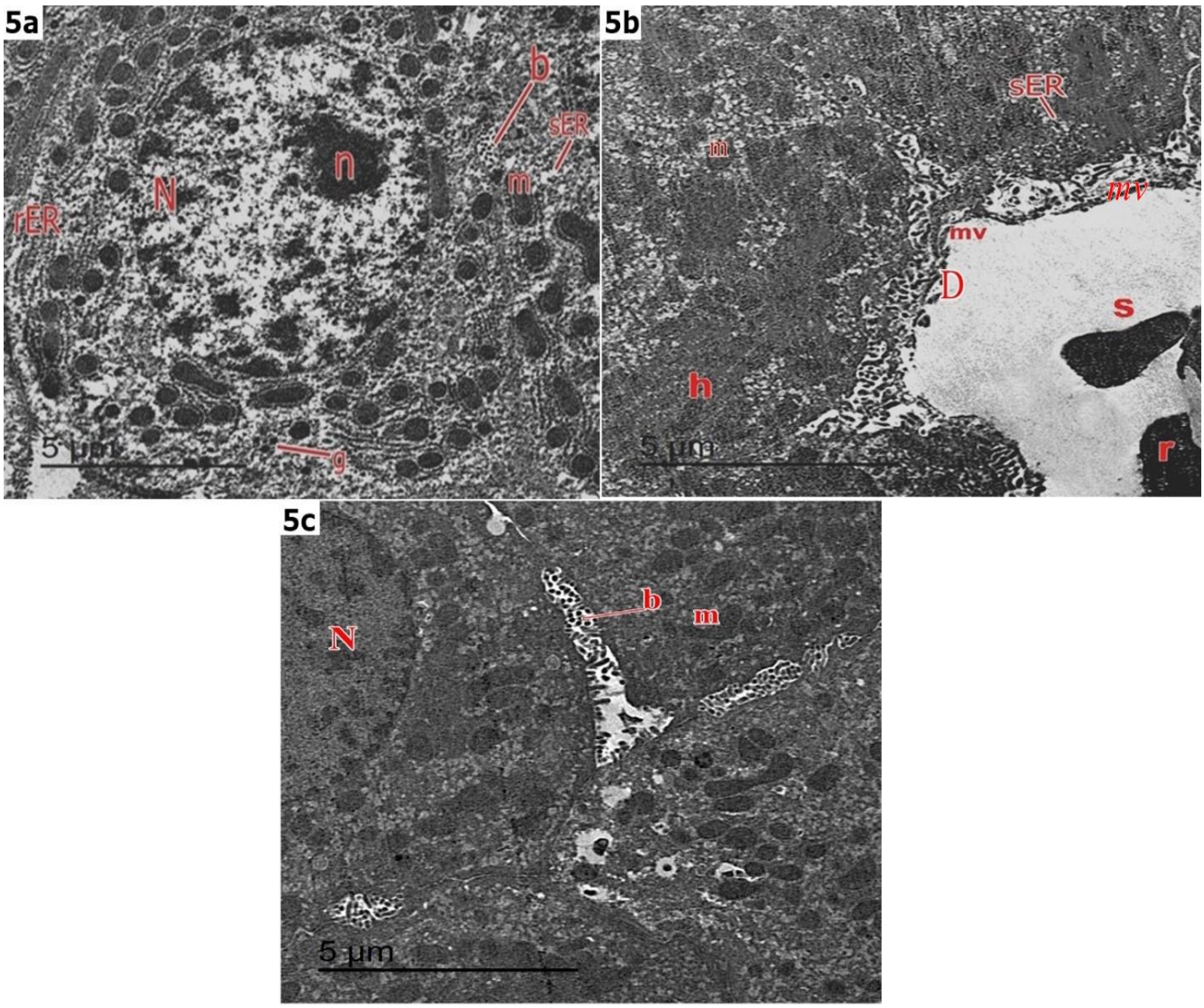

Figure (5): Electron micrographs of ultrathin sections of the left lobe of liver tissue of the **control group**:
5a: Showing a hepatocyte with euchromatic nucleus **(N)** and prominent nucleolus **(n).** The cytoplasm contains mitochondria **(m)**, rough endoplasmic reticulum **(rER)**, smooth endoplasmic reticulum **(sER)** and glycogen granules **(g)**. Bile canaliculi **(b)** between hepatocytes are also observed. **(Mic. Mag. X 10600)**
5b: Showing space of Disse **(D)** located between the hepatocytes **(h)** and blood sinusoids **(S).** The hepatocytes exhibit numerous microvilli **(mv).** smooth Endoplasmic Reticulum **(sER)** and mitochondria **(m)** in the cytoplasm. Blood sinusoids with red blood cells **(r)** are detected **(Mic. Mag. X 13000)**
5c: Showing a portion of hepatocyte with euchromatic nucleus **(N),** bile canaliculi **(b)** are present between hepatocytes, and mitochondria **(m)** are also observed. **(Mic. Mag. X 13000)**

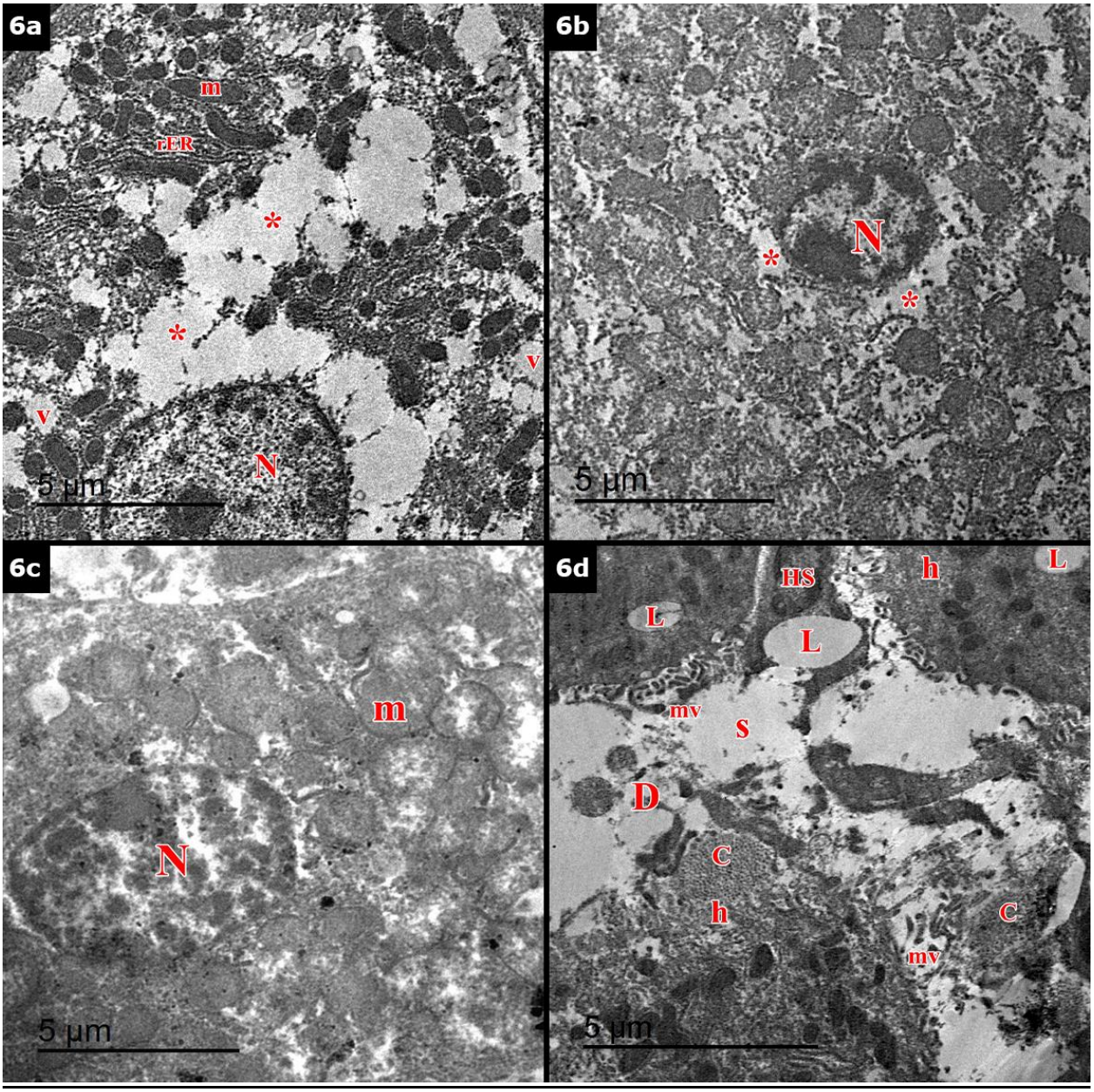

Figure (6): Electron micrographs of ultrathin sections of the left lobe of liver tissue of **high-fat diet (HFD) group:**
6a: Showing portion of hepatocyte with its nucleus **(N).** Its cytoplasm shows vacuoles **(V),** rough endoplasmic reticulum **(rER),** and Mitochondria **(m)** separated by areas of rarefied cytoplasm **(star)** are observed. **(Mic. Mag. X 10600)**
6b: Showing hepatocyte with shrunken apoptotic nucleus **(N)** and its cytoplasm exhibits areas of rarefication **(star)**. **(Mic. Mag. X 10600)**
6c: Showing hepatocyte with heterochromatic nucleus **(N)** and the cytoplasm reveals numerous swollen mitochondria **(m)** with disrupted cristae. **(Mic. Mag. X 10600)**
6d: Showing part of hepatocytes **(h)**, hepatic sinusoids **(S),** and space of Disse **(D).** Hepatocytes exhibit fewer and disrupted microvilli **(mv)** and cytoplasmic lipid droplets **(L)**. Many collagen fibers **(C)** appear in the space of Disse. Hepatic stellate cell **(HS)** with lipid droplets **(L)** in its cytoplasm is also noticed. **(Mic. Mag. X 13000)**

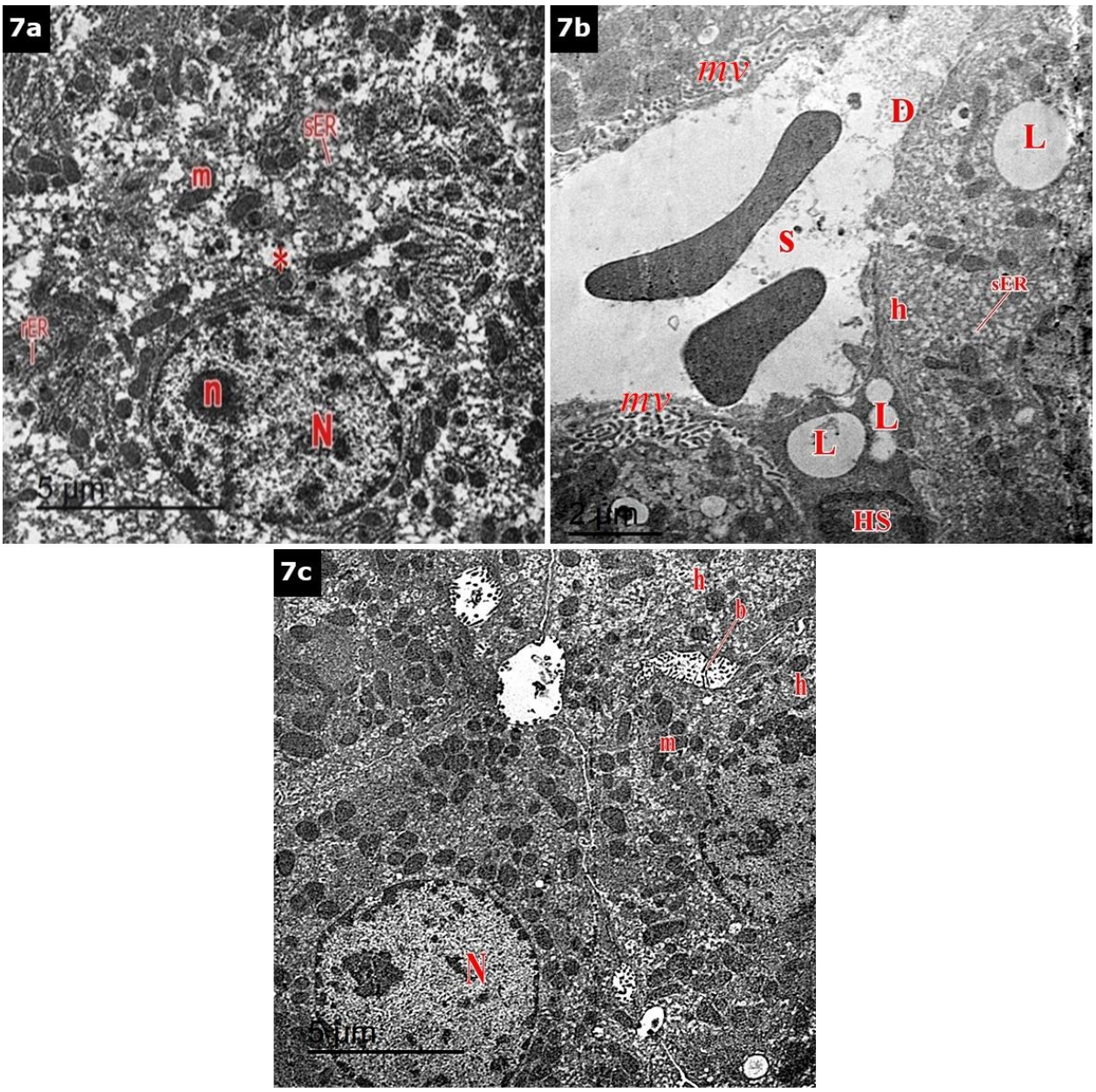

Figure (7): Electron micrographs of ultrathin sections of the left lobe of liver tissue of **high-fat diet +liraglutide group:**
7a: Showing hepatocyte with euchromatic nucleus **(N)** and prominent nucleolus **(n).** The hepatocyte has a few areas of rarefied cytoplasm **(star).** The cytoplasm contains mitochondria **(m),** rough endoplasmic reticulum **(rER)** cisternae, and smooth endoplasmic reticulum **(sER)** are also seen. **(Mic. Mag. X 10600)**
7b: Showing part of hepatocytes **(h)**, hepatic sinusoid **(S),** and space of Disse **(D)**. Hepatocyte cytoplasm contains dilated smooth endoplasmic reticulum **(sER)** and some cytoplasmic lipid droplets **(L)**. Numerous microvilli **(mv)** projecting into the space of Disse **(D)** and hepatic stellate cell **(HS)** with multiple lipid droplets **(L)** in its cytoplasm are also noticed. **(Mic. Mag. X 13000)**
7c: Showing portions of multiple hepatocytes with euchromatic nucleus **(N),** bile canaliculi **(b)**in between hepatocytes **(h),** and mitochondria **(m)** are also seen in the cytoplasm of the hepatocytes. **(Mic. Mag. X 8800)**

DISCUSSION

Non-alcoholic fatty liver disease (NAFLD) is one of the main illnesses that has become nowadays widely spread especially in the Middle East and Western nations. This high prevalence results in a significant clinical and financial strain, as well as a

diminished quality of life concerning health **[17]**. Liraglutide, which is a glucagon-like peptide-1 (GLP-1) receptor agonist has garnered consideration for its positive impacts on metabolic indicators in situations such as type 2 diabetes and obesity [**18]**. Thus, the objective of this research was to assess the biochemical, histological, and immunohistochemical alterations brought on by a high-fat diet that resulted in nonalcoholic fatty liver disease (NAFLD) in adult male albino rats and to look into potential protective effects of liraglutide.

In the present study, the HFD group showed a significant increase in final BMI and final AC compared to the control group. These findings were in agreement with the results of **Naguib et al. [19] and Habib et al. [20].** According to **Zakaria et al. [21]**, the accumulation of both subcutaneous and visceral fats due to HFD leads to an increase in BMI and AC. However, comparing the HFD + liraglutide group to the control group, there was no statistical difference in both parameters. These results are confirmed by **Shamardl et al.'s** explanation **[22]** that liraglutide improves metabolic parameters and enhances fat oxidation rather than storage.

Biochemically, in the HFD group, ALT and AST levels were significantly increased compared to the control group. These findings support the association between HFD and liver injury, and this was agreed with **Reda et al. [23]. Abo-Zaid et al. [24]** suggested that elevated levels of ALT and AST enzymes indicate liver damage and the liver's excessive fat buildup results in oxidative stress. Conversely, there was a non-significant difference between the HFD + liraglutide group and the control group, suggesting that the liver was protected against inflammation and injury. These outcomes were validated **by Jin et al. [25] and Fang et al. [26]. Guo et al. [27]** ascribed this to the suppression of ferroptosis and the initiation of the AMP-Activated Protein Kinase / Acetyl-CoA Carboxylase (AMPK/ACC) signaling pathway.

Concerning lipid profiles, the HFD group showed a highly significant increase in triglycerides (TG), total cholesterol (TC), and low-density lipoprotein (LDL), as well as a decrease in high-density lipoprotein (HDL) levels indicating disrupted lipid metabolism (dyslipidemia). These outcomes were accepted by **Habib et al. [20] & Reda et al. [23].** HFD developed significant hyperlipidemia due to excess energy storage in the form of triglycerides. Also, impaired lipid clearance and imbalances in triglyceride synthesis and release further exacerbated the hyperlipidemia **[28].**

On the contrary, there was no statistically significant difference between the HFD + liraglutide group and the control group, which was in line with **Li et al. [29]. Yang et al. [30]** reported that liraglutide reduces both TG and TC through the enhancement of insulin sensitivity, thereby reducing hepatic triglyceride synthesis and decreasing the availability of free fatty acids for re-esterification. It also promotes fatty acid oxidation and delays gastric emptying, which moderates postprandial lipid spikes**. Gao et al. [31]** suggested that liraglutide has the potential to decrease oxidative stress and inflammation within the liver, attributed to its ability to increase hepatic adiponectin levels. The protein adiponectin, which is released by fat cells, helps control the metabolism of fat and glucose and shields the liver against steatosis and inflammation.

The *HFD group showed altered hepatic architecture whereas most hepatocytes displayed numerous cytoplasmic vacuoles and darkly stained nuclei. Others had deeply acidophilic cytoplasm.* **Leow et al. [32]** attributed these cytoplasmic vacuolations to hepatic steatosis, which can be categorized as macrovesicular or microvesicular steatosis. Macrovesicular steatosis refers to deviations in the delivery, export, synthesis, and metabolism of lipids. On the other hand, microvesicular steatosis is related to defective beta-oxidation of fatty acids and mitochondrial degeneration. Additionally, ***Atta et al. [33] and Hirata et al. [34]*** *discovered that oxidative stress, which affects cell and organelle membranes, has been linked to cytoplasmic vacuolation and lipid peroxidation.*

Li et al. [35] suggested that the deeply acidophilic stained cytoplasm of some hepatocytes in HFD group sections may be due to an increased load of proteins and lipids requiring processing in the endoplasmic reticulum. When the endoplasmic reticulum is unable to handle this increased load, it may result in the buildup of improperly folded proteins. It may result in the buildup of improperly folded proteins. **Leow et al. [32]** found by examination of the ultrathin section that there were swollen mitochondria with disrupted cristae in the cytoplasm of hepatocytes. It was proposed that the presence of megamitochondria indicates either cellular damage or an adaptive response linked to lipid peroxidation. Additionally, acidophilic cytoplasm was characterized as a consequence of the enlargement of mitochondria.

Additionally, the HFD group showed dark staining of nuclei of hepatocytes, which was confirmed at the

ultrastructural level by chromatin condensation and shrunken apoptotic nuclei. This finding was further supported by intense immunoreactions in the cytoplasm of most hepatocytes for caspase 3 and a significant increase in the area percent of its morphometrical statistical finding. These results support **Ruan et al.'s [36]** proposal that excessive fat buildup in the liver can cause oxidative stress, endoplasmic reticulum stress, and mitochondria-mediated apoptosis. The hepatocytes of the same group showed dilated endoplasmic reticulum (ER). **Upadhyay et al. [37]** suggested that two major apoptotic pathways converge on caspases; Intrinsic (Mitochondrial Pathway) involves the release of cytochrome c from damaged mitochondria, leading to caspase-9 activation. Extrinsic (death receptor Pathway) implicates the activation of caspase-8 by death receptors like TNFR1. Both pathways lead to activation of executioner caspases (e.g., caspase-3 and caspase-7), which degrade cellular components and cause apoptosis. **Jayakumar et al. [38]** reported that the endoplasmic reticulum is a vital cellular organelle that significantly contributes to lipid metabolism. This includes processes such as the formation of fat droplets and very-low-density lipoproteins, as well as the synthesis of sphingolipids. Furthermore, it plays a key role in mechanisms related to stress response. **Chen et al. [39]** further elucidated that ER stress is the cause of the smaller apoptotic nuclei observed in the HFD group. Eating a lot of fat can cause misfolded proteins to build up in the ER, which can set off the unfolded protein response (UPR). Extended endoplasmic reticulum stress can trigger programmed cell death via apoptotic mechanisms.

In this study, the HFD group showed also dilated hepatic sinusoids and dilated congested branches of portal veins. **Ma et al. [40]** also found similar results and suggested that excess fatty acids in hepatocytes lead to oxidative stress, mitochondrial dysfunction, and lipid peroxidation. This buildup can also cause the deposition of extracellular matrix components, causing narrowing of the portal vein lumen and increased resistance to blood flow and portal hypertension, ultimately contributing to portal vein congestion. The same group showed swollen mitochondria with disrupted cristae and areas of rarefaction in the cytoplasm of hepatocytes. Also, hepatocytes had few disrupted microvilli in the spaces of Disse, and this finding was agreed with **Sorour et al. [41]. Li et al. [35]** discovered that substantial alterations to the liver, such as enlarged and damaged mitochondria and the development of giant mitochondria, resulted from the high-fat diet attributed to the Na+/K+ pump malfunctions with elevated intracellular sodium and water retention. Additionally, intracellular ATP is reduced when mitochondrial activity is reduced. Consequently, the microvilli separated from the hepatocytes and the hepatocellular ballooning with rarified cytoplasm occurred. **Hassan et al. [42]** proposed that the rarefaction of the cytoplasm might result from the proliferation of smooth endoplasmic reticulum and glycogen accumulation. **Kawai et al. [43]** reported that rarefaction is due to chronic inflammation induced by HFD which activates inflammatory pathways, causing hepatocellular damage.

In the current study, HFD stained sections revealed proliferated several bile ducts in the portal areas and this finding was consistent with **Sato et al. [44]** and **He et al. [45]**. They named this result ductular reaction (DR) which occurs as a compensatory reaction associated with liver injury. **Marakovits and Francis [46]** reported that DR and fibrosis are hallmarks of many liver diseases. Liver fibrosis results from the increased accumulation of collagen produced by myofibroblasts, while ductular reaction (DR) refers to excessive bile duct formation, during liver damage. Various other cell types, such as hepatic stellate cells, hepatocytes, hepatic progenitor cells, mesenchymal stem cells, and immune cells, play a role in both DR and fibrosis through direct or indirect interactions with myofibroblasts and cholangiocytes.

Sirius red-stained sections from the HFD group showed abundant deposition of collagen fibers in the portal areas and around central veins and blood sinusoids. A statistical analysis of morphometric investigation verified a highly significant increase in area percent of collagen fibers compared to the control group. Furthermore, excess collagen fibers were seen at the ultrastructural level in the Disse spaces. These results align with research done by **Lasker et al. [47] and Elkattawy et al. [48].** In a study conducted in **2021, Ortiz and colleagues** established a connection between liver fibrosis and the proliferation and differentiation of hepatic stellate cells (HSCs) into myofibroblast-like cells. This process leads to the excessive deposition of extracellular matrix. The authors also observed that the transformation of HSCs from a quiescent to an activated phenotype takes place two weeks before the onset of fibrosis. Hepatic stellate cells are recognized by their cytoplasmic lipid droplets and cytoskeletal filaments. The number of GFAP-positive cells in the current study was significantly higher than in the

control group, as indicated by GFAP detection (HSC marker). These results were corroborated by **Hassan et al. [42]. Chen et al. [49]** demonstrated how GFAP expression in the liver is connected to inflammatory infiltration and fibrotic liver through cytokine production by activated HSCs. They also proposed a link between elevated reactive oxygen species and HSC activation (ROS). **Roehlen et al. [50]** noted that the activation of hepatic stellate cells (HSCs) is influenced by a range of cytokines, such as transforming growth factor (TGF)-β, tumor necrosis factor (TNF)-α, and platelet-derived growth factor (PDGF), along with additional factors released from injured hepatocytes and activated Kupffer cells.

This study found that concurrent administration of liraglutide in the HFD+ liraglutide group resulted in fewer obvious changes compared to the HFD group observed previously. Moreover, no significant differences in comparison with the control group with the preservation of normal histological hepatic structures were recorded, with only a few hepatocytes still displaying cytoplasmic vacuoles. Similar findings were reported by **Nour et al. [51].** According to **Fang et al. [26],** liraglutide treatment protects hepatocytes, reduces steatosis through autophagy, and helps maintain or restore the liver's normal architecture. **Nevola et al. [52]** found that liraglutide improves insulin sensitivity and increases insulin secretion from pancreatic beta cells. This is important in NAFLD, as insulin resistance is a key influence in hepatic steatosis development. It enhances insulin sensitivity, decreases the production of glucose in the liver and the influx of free fatty acids, and decreases vacuoles and lipid accumulation. Hepatocytes in this group have mitochondria, dilated smooth endoplasmic reticulum, and few areas of rarefication in their cytoplasm. In Disse spaces, hepatocytes exhibited numerous microvilli and some lipid droplets. **Yang et al. [53]** also published comparable findings. Furthermore, liraglutide has been reported by **Ninčević et al. [54]** to reduce the production of reactive oxygen species (ROS) while enhancing the function of antioxidant enzymes. This reduction in oxidative stress prevents liver cell damage and supports overall liver health. The drug's ability to improve mitochondrial function further contributes to the reduction of oxidative stress and better fatty acid metabolism.

Furthermore, the HFD+ liraglutide group showed a moderate amount of collagen fiber deposition. Morphometrical and statistical analysis revealed a highly significant decrease in the area percent of collagen fibers compared to the HFD group. These findings align with the research of **Duparc et al. [55]. Tan et al. [56]** stated that liraglutide has anti-inflammatory and antioxidant properties. It can reduce liver inflammation by decreasing the accumulation of pro-inflammatory macrophages, which may contribute to liraglutide's role in protecting against liver fibrosis.

Concerning, GFAP immunoreactivity in the HFD+ liraglutide group showed moderate reactions in some HSCs. Cell counts of hepatic stellate cells of GFAP immune reaction numbers were highly significantly decreased compared to the HFD group, with no significant differences with the control group. **Petrovic et al. [57]** suggested that liraglutide has been associated with a reduction in oxidative stress, which is a key factor in liver injury and fibrosis. It prevents the activation and proliferation of HSCs.

In the same group, there were moderate immune reactions of caspase 3 in some hepatocytes that showed a highly significant decrease compared to the HFD group. Additionally, there were no significant differences compared to the control group. This finding is consistent with **Li et al. [29],** who found that liraglutide decreases endoplasmic reticulum (ER) stress, a common inducer of apoptosis in hepatocytes, leading to reduced apoptosis. The same study also suggested that liraglutide can decrease apoptosis by reducing oxidative stress and regulating apoptotic genes.

In conclusion, Liraglutide is a promising medication for non-alcoholic fatty liver disease (NAFLD) prevention due to its several mechanisms. It can influence lipid and glucose metabolism, lower oxidative stress and inflammation, and enhance metabolic parameters. Its anti-inflammatory effects and direct hepatic actions make it a comprehensive treatment option. The current study results show that administering liraglutide alongside a high-fat diet can protect the liver from the biochemical and histopathological changes caused by the diet. Further research is recommended to understand the molecular mechanisms of liraglutide's protective effects, optimize dosage for preventive use, and assess long-term safety and efficacy.

Conflict of Interest: None

Financial Disclosures: None

REFERENCES

1. Berthoud HR, Morrison CD and Münzberg H. The obesity epidemic in the face of homeostatic body weight regulation: What went wrong and how can it be fixed?. Physiol. Behav. 2020; 222: 112959-69.
2. Han Y, Wu H, Sun S, Zhao R, Deng Y, Zeng S, et al. Effect of High Fat Diet on Disease Development of

Polycystic Ovary Syndrome and Lifestyle Intervention Strategies. Nutr. 2023; 15(9):2230-44.

3. Pouwels S, Sakran N, Graham Y, Leal A, Pintar T, Yang W, et al. Non-alcoholic fatty liver disease (NAFLD): a review of pathophysiology, clinical management and effects of weight loss. BMC Endocr. Disord. 2022; 22(1): 1-9.
4. Huang X, Chen H, Wen S, Dong M, Zhou L, et al. Therapeutic Approaches for Nonalcoholic Fatty Liver Disease: Established Targets and Drugs. Diabetes Metab Syndr Obes. 2023; 1809-19.
5. Jeeyavudeen MS, Khan SK, Fouda S and Pappachan, JM. Management of metabolic-associated fatty liver disease: The diabetology perspective. World J Gastroenterol. 2023; 29(1): 126.- 43
6. Smits MM and Holst JJ. Endogenous glucagon-like peptide (GLP)-1 as alternative for GLP-1 receptor agonists: Could this work and how?. Diabetes Metab Res Rev. 2023; 39(8): e3699.
7. Zhang N, Tao J, Gao L, Bi Y, Li P, Wang H, et al. Liraglutide attenuates nonalcoholic fatty liver disease by modulating gut microbiota in rats administered a high-fat diet. Biomed Res. Int. 2020; 2020(1): 1-10.
8. He Y, Ao N, Yang J, Wang X, Jin S and Du J. The preventive effect of liraglutide on the lipotoxic liver injury via increasing autophagy. Ann. Hepatol. 2020; 19(1): 44-52.
9. Park Y, Jang I, Park H, Kim J and Lim K. Hypoxic exposure can improve blood glycemic control in high-fat diet-induced obese mice. Phys Act Nutr. 2020; 24(1): 19-24
10. Rasheed RA, Elshikh MS, Mohamed MO, Darweesh MF, Hussein DS, Almutairi SM, et al. Quercetin mitigates the adverse effects of high fat diet on pancreatic and renal tissues in adult male albino rats. J. King Saud Univ. Sci. 2022; 34(4): 101946.
11. Ding M, Fang Q, Cui Y, Shen Q, Liu Q, Wang P, et al. Liraglutide prevents β-cell apoptosis via inactivation of NOX2 and its related signaling pathway. J Diabetes Complications. 2019; 33(4): 267-77.
12. Konopelniuk V, Falalyeyeva T, Tsyryuk O, Savchenko Y, Prybytko I, Kobyliak N, et al. The correction of the metabolic parameters of msg-induced obesity in rats by 2-[4-(benzyloxy) phenoxy] acetic acid. J. Nutr. Intermed. Metab. 2018; 13: 1-9.
13. Yakaiah V, Dakshinamoorthi A and Kavimani S. Effect of Myristica fragrans extract on total body composition in cafeteria diet induced obese rats. Bioinformation.2019; 15(9): 657-65.
14. Endo S, Uto A, Miyashita K, Sato M, Inoue H, Fujii K, et al. Intermittent Fasting Sustainably Improves Glucose Tolerance in Normal Weight Male Mice Through Histone Hyperacetylation. J Clin Endocrinol Metab. 2023;7(7): 1-16 (bvad082).
15. Bancroft J, Layton C and Suvarna S. Bancroft's Theory and practice of histological techniques. 8th ed., Churchill Livingstone of Elsevier, Philadelphia Ch. 10, 126-38, Ch.12, 153- 75 and Ch. 2018; 21: 434-75.
16. Tizro P, Choi C and Khanlou N. Sample Preparation for Transmission Electron microscopy. Methods Mol.Biol.2019; 1897:417-24
17. Nakatsuka T, Tateishi R and Koike K. Changing clinical management of NAFLD in Asia. Liver Int. 2022; 42(9): 1955-68.
18. Rameshrad M, Razavi B, Lalau J, De Broe M and Hosseinzadeh H. An overview of glucagon-like peptide-1 receptor agonists for the treatment of metabolic syndrome: A drug repositioning. Iran. J. Basic Med. Sci. 2020; 23(5): 556-68.
19. Naguib Y, Samaka R, Rizk M, Ameen O and Motawea S. Countering adipose tissue dysfunction could underlie the superiority of telmisartan in the treatment of obesity-related hypertension. Cardiovasc. Diabetol. 2021; 20: 1-19.
20. Habib M, Khalefa A and Alsemeh A. Vitamin D3 Protects Against Non-Alcoholic Fatty Liver Disease in Rats by Modulating Hepatic Iron Deposition. Egypt. J. Histol. 2023; 46(2): 832-46.
21. Zakaria Z, Othman Z, Suleiman J, Che Jalil N, Ghazali W, Nna V, et al. Hepatoprotective effect of bee bread in metabolic dysfunction-associated fatty liver disease (MAFLD) rats: Impact on oxidative stress and inflammation. Antioxidant. 2021; 10(12): 1-21(2031).
22. Shamardl H, Ibrahim N, Merzeban D, Elamir A, Golam R and Elsayed A. Resveratrol and Dulaglutide ameliorate adiposity and liver dysfunction in rats with diet-induced metabolic syndrome: Role of SIRT-1/adipokines/PPARγ and IGF-1. DARU J. Pharm. Sci. 2023; 31(1): 13-27.
23. Reda D, Elshopakey G, Albukhari T, Almehmadi S, Refaat B, Risha E, et al. Vitamin D3 alleviates nonalcoholic fatty liver disease in rats by inhibiting hepatic oxidative stress and inflammation via the SREBP-1-c/PPARα-NF-κB/IR-S2 signaling pathway. Front. pharmacol. 2023; 14: 1164512.
24. Abo-Zaid O, Moawed F, Ismail E and Farrag M. β-sitosterol attenuates high-fat diet-induced hepatic steatosis in rats by modulating lipid metabolism, inflammation and ER stress pathway. BMC Pharmacol Toxicol. 2023; 24(1): 24-31.
25. Jin M, Niu X, Liu Y, Zhang D, Yuan D and Shen H. Effect of glucagon-like peptide-1 receptor agonists

on adipokine level of nonalcoholic fatty liver disease in rats fed high-fat diet. Open Med. 2020; 15(1): 689-96.

26. Fang Y, Ji L, Zhu C, Xiao Y, Zhang J, Lu J, et al. Liraglutide alleviates hepatic steatosis by activating the TFEB-regulated autophagy-lysosomal pathway. Front. cell dev. biol. 2020; 8: 602574.

27. Guo T, Yan W, Cui X, Liu N, Wei X, Sun Y, et al. Liraglutide attenuates type 2 diabetes mellitus-associated non-alcoholic fatty liver disease by activating AMPK/ACC signaling and inhibiting ferroptosis. Mol. Med. 2023; 29(1): 1-17(132).

28. Abdelmoneim D, El-Adl M, El-Sayed G and El-Sherbini E. Protective effect of fenofibrate against high-fat–high-fructose diet induced non-obese NAFLD in rats. Fundam Clin Pharmacol. 2021; 35(2): 379-88.

29. Li J, Xu J, Zhu F and Wang C. Effective treatment for fatty liver of liraglutide via inhibiting endoplasmic reticulum stress, oxidative stress and apoptosis pathways. Arch Med Res. 2024; DOI: https://doi.org/10.5114/aoms/186658

30. Yang S, Xu R, Cui C, Wang Y, Du Y, Chen Z, et al. Liraglutide downregulates hepatic LDL receptor and PCSK9 expression in HepG2 cells and db/db mice through a HNF-1a dependent mechanism. Cardiovasc. Diabetol. 2018; 17: 1-10.

31. Gao H, Zeng Z, Zhang H, Zhou X, Guan L, Deng W, et al. The glucagon-like peptide-1 analogue liraglutide inhibits oxidative stress and inflammatory response in the liver of rats with diet-induced non-alcoholic fatty liver disease. Biol. Pharm. Bull. 2015; 38(5): 694-702.

32. Leow W, Chan A, Mendoza P, Lo R, Yap K, Kim H. Non-alcoholic fatty liver disease: the pathologist's perspective. Clin Mol Hepatol. 2023; 29(Suppl): S302-S318

33. Atta I, Elnady M, Alghamdi A, Alghamdi A, Aboulata A and Shatla I. Assessing the hepatoprotective effects of hesperidin on liver-associated disorders in albino rats with experimentally induced obesity and type II diabetes: A histological and biochemical study. Heliyon.2023; 9(5):1-14.

34. Hirata Y, Cai R, Volchuk A, Steinberg B, Saito Y, Matsuzawa A, et al. Lipid peroxidation increases membrane tension, Piezo1 gating, and cation permeability to execute ferroptosis. Curr. Biol. 2023; 33(7); 1282-94.

35. Li Y, Zheng T, Xiao S, Wang P, Yang W, Jiang L, et al. Hepatocytic ballooning in non-alcoholic steatohepatitis: Dilemmas and future directions. Liver Int. 2023; 43(6): 1170-82.

36. Ruan L, Li F, Li S, Zhang M, Wang F, Lv X, et al. Effect of Different Exercise Intensities on Hepatocyte Apoptosis in HFD-Induced NAFLD in Rats: The Possible Role of Endoplasmic Reticulum Stress through the Regulation of the IRE1/JNK and eIF2α/CHOP Signal Pathways. Oxid Med Cell Longev. 2021(1): 6378568.

37. Upadhyay, M., & Bonilha, V. L. Regulated cell death pathways in the sodium iodate model: Insights and implications for AMD. Exp. Eye Res, 2023,109728.

38. Jayakumar S, Guillot S, Argo C, Redick J and Caldwell S. Ultrastructural findings in human nonalcoholic steatohepatitis. Expert Rev. Gastroenterol. Hepatol. 2011; 5(2): 141-5.

39. Chen X, Shi C, He M, Xiong S and Xia X. Endoplasmic reticulum stress: molecular mechanism and therapeutic targets. Signal Transduct Target Ther. 2023; 8(1).

40. Ma Y, Lee G, Heo S and Roh Y. Oxidative stress is a key modulator in the development of nonalcoholic fatty liver disease. Antioxidant. 2021; 11(1):1-25.

41. Sorour HA, Salem MA, Abdelmaksoud DA, Elgalil A, Mohamed M. The Impact of High Fat Diet and Flaxseed on Liver Histology, Histochemistry and Morphometry in Ovariectomized Albino Rat. Egypt. J. Histol., 2022; 45(1), 68-89.

42. Hassan N, Soliman G, Okasha E and Shalaby A. Histological, immunohistochemical, and biochemical study of experimentally induced fatty liver in adult male albino rat and the possible protective role of pomegranate. J. Microsc. Ultrastruct. 2018; 6(1): 44-55.

43. Kawai T, Autieri M and Scalia R. Adipose tissue inflammation and metabolic dysfunction in obesity. Am. J. Physiol. Cell Physiol. 2021; 320(3): C375-C91.

44. Sato K, Marzioni M, Meng F, Francis H, Glaser S and Alpini G. Ductular reaction in liver diseases: pathological mechanisms and translational significances. Hepatol 2019; 69(1): 420-430.

45. He Y, Pan J, Xu L, Gu T and Chen Y. Ductular reaction in non-alcoholic fatty liver disease: When Macbeth is perverted. World J of Hepatol. 2023;15(6): 725-740.

46. Marakovits C, and Francis H. Unraveling the complexities of fibrosis and ductular reaction in liver disease: Pathogenesis, mechanisms, and therapeutic insights. Am J of Physiol-Cell Physiol. 2024; 326(3):698-706.

47. Lasker S, Rahman M, Parvez F, Zamila M, Miah P, Nahar K, et al. High-fat diet-induced metabolic syndrome and oxidative stress in obese rats are

ameliorated by yogurt supplementation. Sci. Rep. 2019; 9(1): 20026.

48. Elkattawy H, Elsherbini D, Ebrahim H, Abdullah D, Al-Zahaby S, Nosery Y, et al. Rho-kinase inhibition ameliorates non-alcoholic fatty liver disease in type 2 diabetic rats. Physiol. Res. 2022; 71(5): 615-630.

49. Chen Z, Tian R, She Z, Cai J and Li H. Role of oxidative stress in the pathogenesis of nonalcoholic fatty liver disease. Free Radic Biol Med. 2020; 152: 116-41.

50. Roehlen, N., Crouchet, E., & Baumert, T. F. Liver fibrosis: mechanistic concepts and therapeutic perspectives. Cells, 2020, 9(4), 875. /

51. Nour S, Sakara M, Hasanin Z and Hamed S. Histological and immunohistochemical study of the effect of liraglutide in experimental model of non-alcoholic fatty liver disease. Egypt. j. basic appl. sci..2023; 10(1): 342-57.

52. Nevola R, Epifani R, Imbriani S, Tortorella G, Aprea C, Galiero R, et al. GLP-1 receptor agonists in non-alcoholic fatty liver disease: current evidence and future perspectives. Int. J. Mol. Sci. 2023; 24(2): 1703.

53. Yang J, Ao N, Du J, Wang X and He Y. Protective effect of liraglutide against ER stress in the liver of high-fat diet-induced insulin-resistant rats. Endocr. 2015; 49: 106-18.

54. Ninčević V, Zjalić M, Kolarić T, Smolić M, Kizivat T, Kuna L, et al. Renoprotective effect of liraglutide is mediated via the inhibition of TGF-beta 1 in an LLC-PK1 cell model of diabetic nephropathy. Curr. Issues Mol. Biol. 2022; 44(3):1087-114.

55. Duparc T, Briand F, Trenteseaux C, Merian J, Combes G, Najib S, et al. Liraglutide improves hepatic steatosis and metabolic dysfunctions in a 3-week dietary mouse model of nonalcoholic steatohepatitis. Am. J. Physiol. Gastrointest. Liver Physiol. 2019; 317(4): G508-G17.

56. Tan Y, Zhen Q, Ding X, Shen T, Liu F, Wang Y, et al. Association between use of liraglutide and liver fibrosis in patients with type 2 diabetes. Front. Endocrinol. 2022; 13: 935180.

57. Petrovic A, Igrec D, Rozac K, Bojanic K, Kuna L, Kolaric T, et al. The role of GLP1-RAs in direct modulation of lipid metabolism in hepatic tissue as determined using in vitro models of NAFLD. Curr. Issues Mol. Biol. 2023; 45(6): 4544-56.

Figure A1: mean values of BMI in studied groups

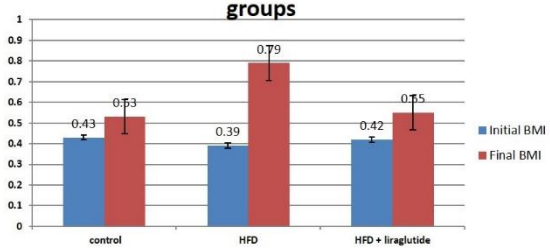

Figure A2: mean values of abdominal circumferences in studied groups

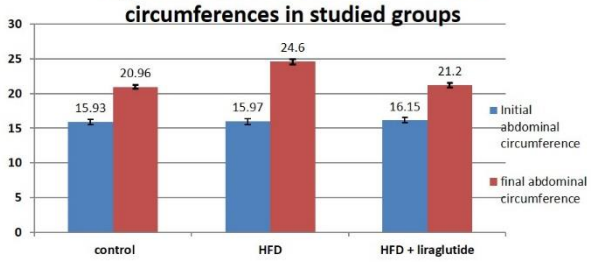

Figure A3: mean values of serum (ALT, AST) in studied groups

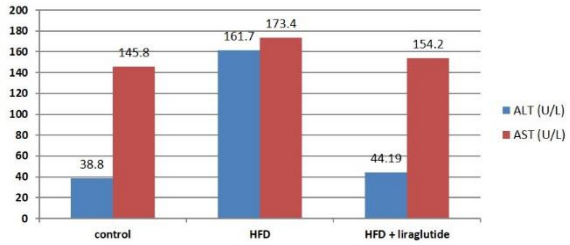

Figure A4: mean values of serum lipid profiles in studied groups

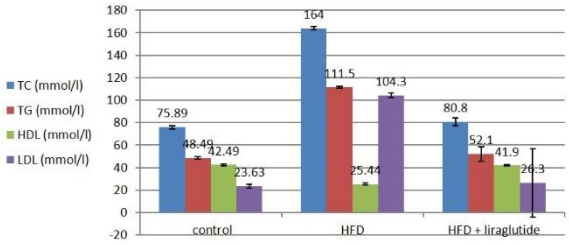

Figure (A): Comparison between different studied groups regarding BMI, abdominal circumference, ALT, AST and lipid profiles.

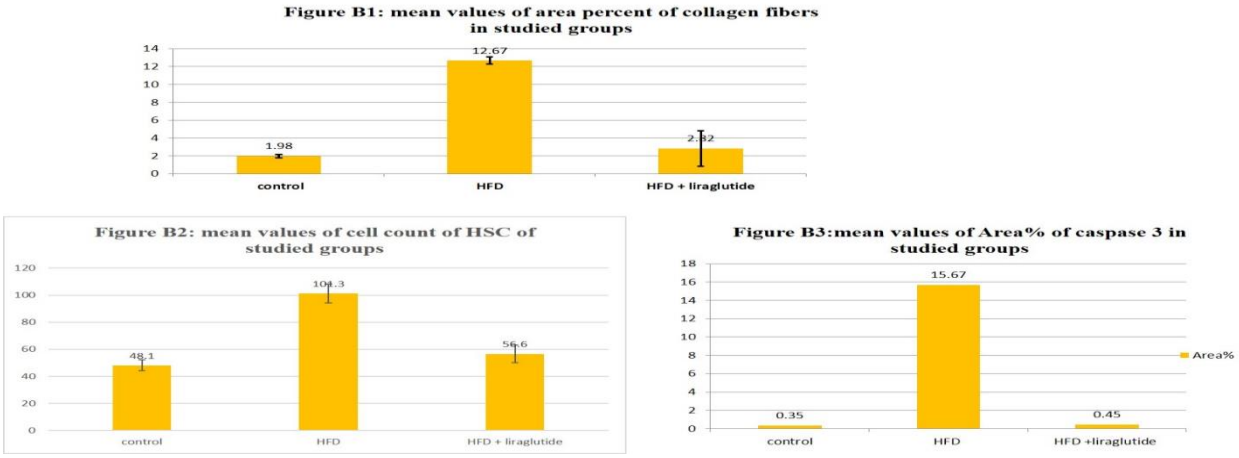

Figure (B): Comparison between different studied groups regarding area percent of collagen fibers distribution, cell count of HSC and area % of caspase 3.

ALT: Alanine aminotransferase, AST: Aspartate aminotransferase TC: total cholesterol, TG: triglyceride, HDL: High-density lipoprotein, LDL: low-density lipoprotein * p>0.05 is no statistically significant **p≤0.001 is statistically highly significant SD: Standard deviation, HFD: high fat diet P1: control with HFD P2: control with HFD +liraglutide

P3: HFD with HFD +liraglutide

Citation

Shaban, S., Mohamed, D., Mahmoud, A., Abdel-aziz, H. Exploring the Cytoprotective Role of Liraglutide in Non-Alcoholic Fatty Liver Disease Experimentally Induced in the Rat Model (Histological and Biochemical Study). ***Zagazig University Medical Journal*****, 2024; (4348-4366): -. doi: 10.21608/zumj.2024.321384.3582**